EUROPEAN FUSION DEVELOPMENT AGREEMENT

EFDA–JET–PR(05)18

P. Mantica, D. Van Eester, X. Garbet, F. Imbeaux, L. Laborde, M. Mantsinen, A. Marinoni, D. Mazon, D. Moreau, A. Thyagaraja, N. Hawkes, E. Joffrin, V. Kiptily, P.J. Knight, S. Pinches, A. Salmi, S. Sharapov, I. Voitsekhovitch, P. de Vries, K.-D. Zastrow and JET EFDA contributors

New Evidence on Internal Transport Barrier Physics from Heat Pulse Propagation in JET

New Evidence on Internal Transport Barrier Physics from Heat Pulse Propagation in JET

P. Mantica[1], D. Van Eester[2], X. Garbet[3], F. Imbeaux[3], L. Laborde[3], M. Mantsinen[4], A. Marinoni[5,#], D. Mazon[3], D. Moreau[3], A. Thyagaraja[6], N. Hawkes[6], E. Joffrin[3], V. Kiptily[6], P.J. Knight[6], S. Pinches[7], A. Salmi[4], S. Sharapov[6], I. Voitsekhovitch[6], P. de Vries[8], K.-D. Zastrow[6] and JET EFDA contributors*

[1]*Istituto di Fisica del Plasma 'P.Caldirola', Associazione Euratom-ENEA-CNR, Milano, Italy*
[2]*LPP-ERM/KMS, Association Euratom-Belgian State, TEC, B-1000 Brussels, Belgium*
[3]*Association Euratom-CEA, CEA Cadarache, St Paul-lez-Durance Cedex, France*
[4]*Helsinki University of Technology, Association Euratom-Tekes, P.O.Box 2200, Finland*
[5]*Politecnico di Milano, Dipartimento di Ingegneria Nucleare, Milano , Italy*
[6]*EURATOM/UKAEA Fusion Association, Culham Science Centre, Abingdon, OX14 3DB, UK*
[7]*Max-Planck-Institut für Plasmaphysik, EURATOM Association, Garching, Germany*
[8]*FOM Institute for Plasma Physics Rijnhuizen, Euratom-FOM Association, Nieuwegein, The Netherlands*
[#]*Present address: EPFL, CRPP-Euratom Association, CH 1015, Lausanne , Suisse*
** See annex of J. Pamela et al, "Overview of JET Results ", (Proc.20 th IAEA Fusion Energy Conference, Vilamoura, Portugal (2004).*

Preprint of Paper to be submitted for publication in
Plasma Physics and Controlled Fusion

“This document is intended for publication in the open literature. It is made available on the understanding that it may not be further circulated and extracts or references may not be published prior to publication of the original when applicable, or without the consent of the Publications Officer, EFDA, Culham Science Centre, Abingdon, Oxon, OX14 3DB, UK.”

“Enquiries about Copyright and reproduction should be addressed to the Publications Officer, EFDA, Culham Science Centre, Abingdon, Oxon, OX14 3DB, UK.”

ABSTRACT

First experimental results of electron temperature modulation experiments in plasmas characterized by strong and long–lasting electron and ion Internal Transport Barriers (ITB) have been obtained in JET using ICRH in the Mode Conversion scheme. The ITB is shown to be a well localized narrow layer with low heat diffusivity, characterized by sub-critical transport and loss of stiffness. In addition, results from cold pulse propagation experiments suggest a second order transition process for ITB formation and can be reproduced by non-linear fluid turbulence simulations.

INTRODUCTION

Power modulation experiments are a well known tool to probe electron heat transport in fusion grade plasmas and have been widely used in conventional L- or H-mode scenarios to assess the physics of turbulence driven transport [1-5]. On the other hand, several key questions remain unsolved on the physics of formation of Internal Transport Barriers (ITB), i.e. regions where turbulence is quenched and transport greatly reduced [6,7]. Amongst these questions, the type of transition mechanism, the ITB spatial localization and transport properties, the respective roles of the ExB flow shear and magnetic shear and the role of rational magnetic surfaces. In this paper, new results are presented of power modulation experiments in JET plasmas characterized by strong electron and ion ITBs, which provide new evidence on some of these issues. These experiments are complemented by previous results of cold pulse propagation from the edge into the ITB [8], which have now been addressed by new theoretical activity and turbulence simulations.

The JET tokamak (R=2.96m, a=1 m) offers good capabilities for perturbative studies of ITBs: the use of Lower Hybrid (LH) preheat to create a slowly evolving strongly reversed safety factor (q) profile and induce long lasting ITBs sustained by large NBI power [9], the availability of a space and time resolved electron temperature (T_e) ECE diagnostic, the possibility to use as a transport probe the modulated RF ICRH power in Mode Conversion (MC) scheme, as an alternative to the more commonly used ECH (not available in JET). This deposition scheme, which takes place in D plasmas with ^{3}He concentrations of 10-20% [10,11], provides a source of direct, localized and controllable power to electrons, suitable for electron transport studies and already successfully used in JET conventional scenarios [3,4].

JET plasmas with toroidal field B_T~3.25-3.6 T, plasma current I_p~2.6-2.9MA (q_{95}~5), elongation k_a~1.75, triangularity δ~0.25 (averaged lower and upper) and density n_{eo}~3-5 10^{19}m^{-3} have been used as targets. LH power ~2-3MW was applied in the preheat phase (t = 2-4s). Then, from t = 4s to 10s, up to 18MW of NBI power and 4MW of ICRH power modulated with half depth at 15-45Hz with duty cycle ~60% were applied. Figure 1 shows contour plots of ∇T_e for one of the best shots. The ITB is located in the region of negative magnetic shear.

Two RF deposition schemes have been explored: a) ^{3}He concentration~12% (mixed minority heating and MC), which led to the best ITB performance (Figure 2: T_{i0}~24 keV, T_{e0}~13 keV, n_{e0}~5 10^{19} m^{-3}, at an additional total power level of 15 MW, with an equivalent Q_{DT}[12]~0.25); b) ^{3}He

concentration~20% (full MC), which allowed the cleanest modulation signals and best transport results (Figure 3). FIGs.2 and 3 show steady-state profiles of T_e, T_i, n_e, q and profiles of amplitudes (A) and phases (φ) of the T_e heat wave at the modulation frequency obtained by standard FFT techniques. The MC power has been localized either at the ITB layer (Figure 2), providing a heat wave generated at the ITB and travelling in two directions away from it, or just outside the ITB (Figure 3), providing a heat wave that travels towards it. Note that in the case of FIG.3 a fraction of the power is also deposited to electrons in the centre via Fast Wave Landau damping, so there are two heat waves propagating towards the ITB, one from the centre and one from the outer region.

Two important questions under debate regarding ITB transport are i) whether the improved confinement is limited to a narrow layer or rather extends to the whole core region inside the ITB foot; ii) whether the ITB is a region of stiff transport [4] characterized by a threshold in R/L_{Te} ($L_{Te} = T_e/\nabla T_e$) larger than in conventional plasmas (case 1) or rather a region below threshold where turbulence is suppressed leading to a loss of stiffness (case 2). These two situations are exemplified in figure 4 within the assumption of a second order transition scheme for ITB formation. This assumption will be justified later. The concept of phase transition can be applied to ITB formation using as order parameter the electron heat flux, whilst the plasma response is R/L_{Te}. 1^{st} order means that R/L_{Te} experiences a discontinuity at the transition (Figure 7 discussed later) while it stays continuous for a 2^{nd} order transition (Figure 4). The two cases in figure4 have profound differences as far as heat propagation is concerned. In fact the damping of the heat wave in the ITB is regulated by the perturbative (incremental) heat diffusivity $\chi_e^{hp} = -\partial q_e / n_e \partial \nabla T_e$ (where q_e is the heat flux), which is much higher in case 1 with respect to case 2. One would therefore expect strong damping of the wave in the ITB in case 2, and propagation of the wave through the ITB in case 1.

Regarding question i), both figures 2 and 3 show sharp discontinuities in the heat wave propagation (i.e. in the slopes of the A and φ profiles) both at the foot and at the top of the high ∇T_e region, indicating that, at least for these reverse shear ITBs, the ITB is indeed a narrow layer with low χ_e embedded in a higher χ_e plasma, and not a general improvement of confinement in the core region. Regarding question ii), Figure 3 shows that the heat wave is strongly damped when meeting the ITB from either side. This is consistent with a situation of complete loss of stiffness due to the plasma having become fully sub-critical with respect to an increased threshold value (case 2). In this case, χ_e does not depend on ∇T_e the perturbative χ_e coincides with the power balance χ_e and is low, the two heat waves are strongly damped and cannot cross the ITB, the phase exhibits a sharp jump. In case 1) instead, corresponding to a situation where the plasma in the ITB is close to marginality and very stiff, with an incremental χ_e very large, the two heat waves would have propagated fast inside ITB with a small phase change and amplitudes not strongly damped, eventually crossing the ITB and getting superimposed. This is clearly at variance with observations.

Attempts to model the ITB modulation results with various transport models have been [3, 13] and still are being carried out. More detailed discussion of such modelling effort will be presented in a separate paper [14]. Empirical models are in general capable of reproducing the main experimental

features using a properly shaped χ_e profile. One example is shown in FIG.5, using a χ_e critical gradient model [4] of the type shown in figure 4:

$$\chi_e = \chi_0 + \chi_s T_e^{3/2} \left(\frac{-R\partial_r T_e}{T_e} - \kappa_e \right) H \left(\frac{-R\partial_r T_e}{T_e} - \kappa_e \right) \quad (1)$$

where χ_0 quantifies the residual transport (not necessarily neoclassical, as there may be other instabilities surviving after stabilization of the one involved in the transition), χ_s provides the stiffness level, κ_c is the threshold for onset of turbulent transport, assumed for sake of simplicity to have a square box profile. The ITB is then a layer completely below threshold, i.e. with low, constant heat diffusivity, embedded in a plasma where turbulent transport with significant stiffness level dominates. This crude model is capable of reproducing the main experimental evidence, although finer refinements, beyond the scope of the present letter, would be needed to match quantitatively all the details of the experimental results. The situation of modeling is even more difficult with regard to first principle models. Unlike for cold pulses, turbulence simulations are not feasible for modulation at 15Hz due to excessive calculation time. The situation of 1D fluid models like GLF23 or Weiland is at present not satisfactory already for reproduction of steady-state [14, 15], so the comparison with the modulation results would not be relevant.

The oversimplification of the model in figure 5 is already evident from a careful analysis of the slopes of A and φ within the ITB in figures 3, 5. One can notice that that the inner ITB portion has higher slopes, indicating that χ_e is not uniform within the ITB, with a lower χ_e (i.e. a stronger stabilization of turbulence) in the inner portion. The outer portion shows reduced χ_e compared to the region outside the ITB, but still higher than in the inner ITB portion. This could correspond to partial stabilization, or to a situation which gets closer to the threshold. In other words the ITB layer gets more fragile in the region near its foot. This observation is in agreement with earlier studies of JET ITBs using cold pulses from the edge induced by Ni laser ablation [8]. The cold pulse showed a growth when meeting the ITB foot (corresponding to transport re-enhanced in the more fragile outer ITB portion) and then a strong damping further inside (Figure 6(a)). This observation was interpreted as an erosion of the less stabilized part of the ITB due to increased ∇T_e associated with the cold wave [8].

This result has now been deeply investigated using two global fluid turbulence codes: the electrostatic TRB [15] and the electromagnetic CUTIE [16]. The results of these simulations are shown in figures 6(b) and (c), and reproduce the growth of the cold pulse when meeting the ITB foot. This behavior is considered a strong indication in favour of a 2nd order transition scheme for ITB formation, of the type shown in FIG.4. In this scheme the transition to ITB is a continuous process involving a threshold value of R/L_{Te}, which can be shifted up for example by the presence of negative magnetic shear or moderate $E\times B$ shear, and does not involve bifurcations or hysteresis. In this framework the cold pulse enhancement in the outer ITB region is easily explained in terms of a re-crossing of the threshold (with associated χ_e increase), due to the enhanced ∇T_e carried by the cold pulse, in a region which is just below the stability threshold. Consistently, no sign of amplification of the modulation heat wave (carrying a decrease in ∇T_e) is observed experimentally when it meets the ITB foot (FIG.3). We note

that recently other pieces of evidence of the continuous character of the ITB formation process have been obtained, in JET [18,19] or in other machines [20].

On the other hand, a 1st order transition scheme would not account for the observed cold pulse growth. This scheme is illustrated in FIG.7, with an S-shaped curve originated by the effect of decorrelation of turbulence eddies due to strong $E \times B$ flow shear, as originally proposed for the edge H-mode barrier formation [21,22], and then de facto extended also to the formation of Internal Barriers. This process is characterized by bifurcation and hysteresis in the back-transition. Some authors have also argued that the critical flux for the 1st order transition should be the same for the forward and backward transition and is determined by an equal area (Maxwell) constraint [23,24], but this does not change our main conclusion. Qualitatively one can see from figure 7 that, once bifurcation has taken place, the ITB is formed and transport has got back to the low transport branch, so that any further increase in ∇T_e is not a destabilizing factor for the ITB. This has been confirmed by numerical simulations [25] using two empirical models for χ_e reproducing the two types of transitions as in figures 4 and 7. The radial boundary layer where the transition takes place is modeled by inclusion of an hyperdiffusivity term [26]. It has been checked that, in the steady-state phase after the ITB formation, the heat flux at the interface between the 2 regions is consistent with the Maxwell construction. Figure8 shows the contour plots of the T_e variation for experiment and for the simulations using the two transitions schemes. Cold pulse enhancement can only be reproduced when the heat diffusivity becomes large in a finite region near the foot of the barrier ($\rho = [0.4 ; 0.5]$). This takes place on cold pulse arrival only in the 2nd order transition case, when the threshold is overcome and the plasma in that region switches back to the turbulent stiff branch. In the 1st order case instead the cold pulse cannot move the plasma away from the ITB branch, and the cold pulse is just damped. Further inside ($\rho = [0.3 ; 0.4]$), the cold pulse is damped either in experiment and in both simulations, which confirms a reduced incremental diffusivity as indicated by the modulation experiments.

ACKNOWLEDGEMENTS

This work was carried out within the framework of the European Fusion Development Agreement. The views and opinions expressed herein do not necessarily reflect those of the European Commission.

REFERENCES

[1]. F. Ryter *et al.,* Phys. Rev. Lett. **86,** 2325 (2001)

[2]. F.Ryter *et al.,* Plasma Phys. Control. Fusion **43**, 323 (2001)

[3]. P.Mantica *et al.*, in *Proc. of the 20th International Conference on Fusion Energy, Vilamoura, 2004* [IAEA, Vienna, 2004], EX/P6-18

[4]. X.Garbet *et al.,* Plasma Phys. Control. Fusion **46,** 1351 (2004)

[5]. J.C.DeBoo *et al.*, in *Proceedings of the 20th Interntional Conference on Fusion Energy, Vilamoura, 2004* [IAEA, Vienna, 2004], EX/P6-13

[6]. J.W.Connor et al., *Nucl. Fusion* **44**, R1 (2004)

[7]. X.Garbet *et al.*, Plasma Phys. Control. Fusion **46,** B557 (2004)
[8]. P.Mantica *et al.*, Plasma Phys. Control. Fusion **44**, 2185 (2002)
[9]. X. Litaudon *et al.*, Plasma Phys. Control. Fusion **44**, 1057 (2002)
[10]. M.Mantsinen et al., Nuclear Fusion 44, 33 (2004)
[11]. D.Van Eester *et al.*, in *Proc. 15th Top. Conf. on RF Power in Plasmas, May 2003, Wyoming, USA*
[12]. J.Wesson, *Tokamaks*, Oxford Science Publications (2004)
[13]. P.Mantica *et al.*, in *Proc. of 31st EPS Conference, London, 2004*, Europhysics Conf. Abstracts 2004 Vol.28G, P1.154
[14]. A. Marinoni *et al.*, to be submitted to Plasma Phys.Control.Fusion
[15]. T.Tala *et al.*, in *Proc. of the 20th International Conference on Fusion Energy, Vilamoura, 2004* [IAEA, Vienna, 2004], TH/P2-9
[16]. X.Garbet *et al.*, Phys. Plasmas **8**, 2793 (2001)
[17]. A. Thyagaraja, *et al.*, Eur. Journ. Mech B/Fluids/B **23,** 475 (2004)
[18]. Y.Baranov *et al.*, accepted for publication in Plasma Phys. Control. Fusion
[19]. G.M.D.Hogeweij et al., to be presented at 32nd EPS Plasma Physics conference, Tarragona, June 2005
[20]. O.Sauter et al., Phys. Rev. Lett. **94,** 105002-1 (2005)
[21]. F.L. Hinton, Phys. Fluids B **3**, 696 (1991)
[22]. P. W. Terry, Rev. Mod. Phys. **72** 109 (2000)
[23]. M.A. Malkov and P.H. Diamond, private communication
[24]. S-I. Itoh, K. Itoh, and S. Toda, Phys. Rev. Lett. **89**, 215001 (2002)
[25]. L. Laborde, D. Mazon, D.Moreau, to be submitted to ., Plasma Phys. Control. Fusion
[26]. V.B. Lebedev and P.H Diamond, Phys Plasmas, **4,** 1087 (1997)

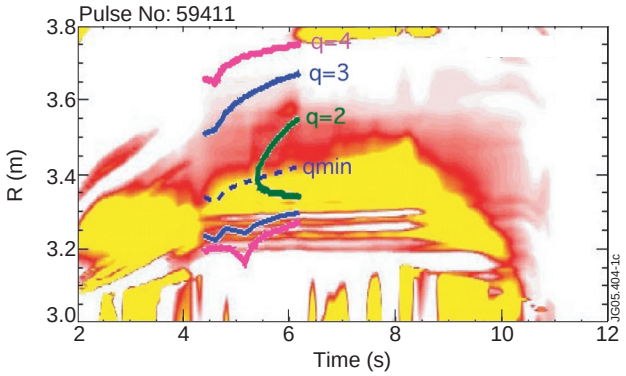

Figure 1: (colors on-line). Contour plots of ∇T_e for Pulse No: 59411 (^{3}He concentration ~12%, ICRH deposition internal to ITB). The yellow region around R=3.3 m indicates the ITB. The locations of minimum q and rational q values from MSE diagnostic are also plotted.

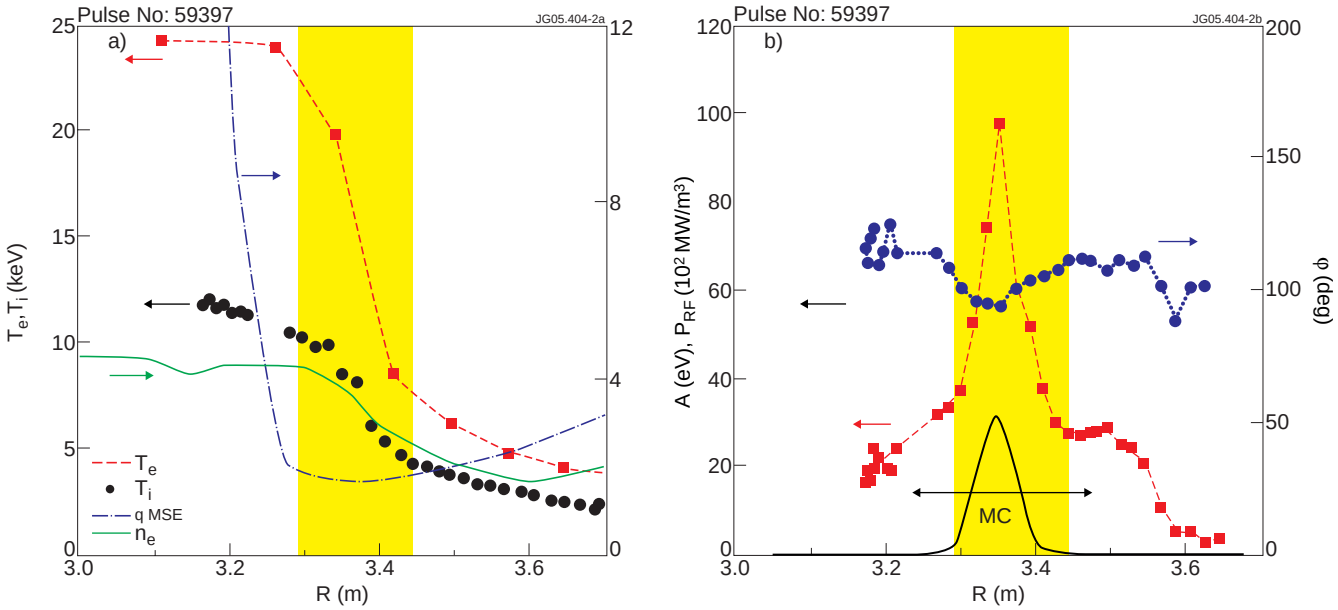

Figure 2: (colors online). a) Experimental profiles at t=8 s (maximum performance) of T_e, T_i, n_e and q for Pulse No: 59397 (3.45T/2.8MA, ^{3}He~12%, ICRH f=33MHz). The ITB region is highlighted. b) profiles of Fourier component of A (red squares) and φ (blue circles) at the modulation frequency (15 Hz) during the time interval 6.2-6.48s. RF power deposition profiles are also plotted (dashed black line).

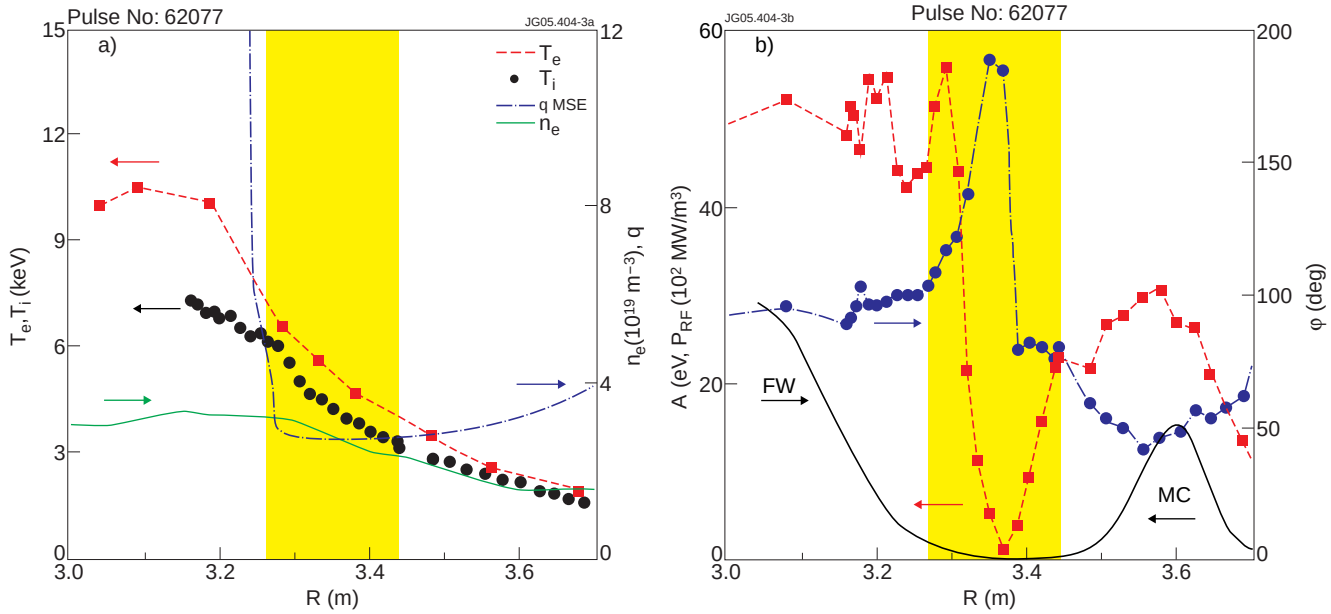

Figure 3: (colors online). a) Experimental profiles at t=5.5s of T_e, T_i, n_e and q for shot 62077 (3.25T/2.6MA, ^{3}He~20%, ICRH f=37MHz). The ITB region is highlighted. b) profiles of Fourier component of A (red squares) and φ (blue circles) at the modulation frequency (20 Hz) during the time interval 5.5-5.7s. RF power deposition profiles are also plotted (dashed black line).

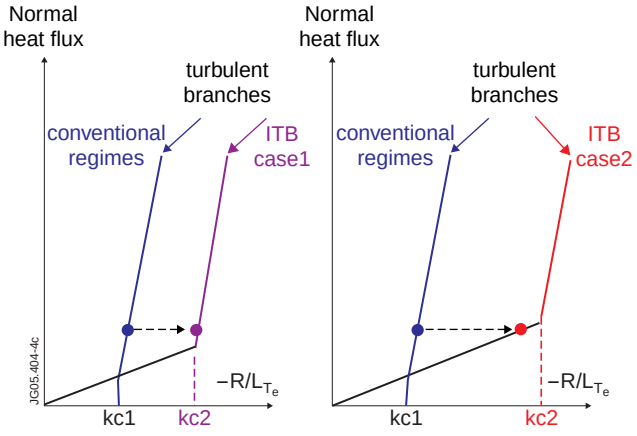

Figure 4: (colors on-line). Schematic of 2nd order transition for ITB formation. The turbulence threshold is higher than in conventional plasmas. Two situations can be hypothesized, as discussed in the text.

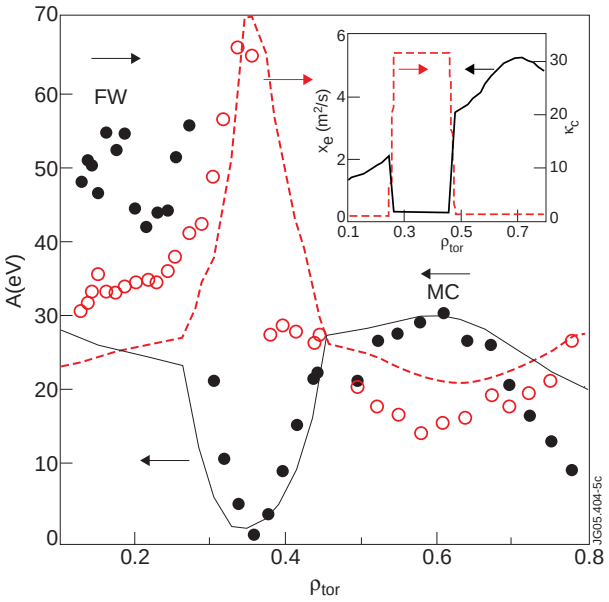

Figure 5: (colors on-line). Experimental (dots) and simulated using the CGM model (lines) profiles of amplitudes (black full symbols) and phases (red open symbols) at fundamental modulation frequency for Pulse No: 62077. In the inset also the χ_e profile (black full line) used in the simulation is plotted at one time during the modulation ON phase, together with the time constant profile of the threshold κ_c (red dashed line).

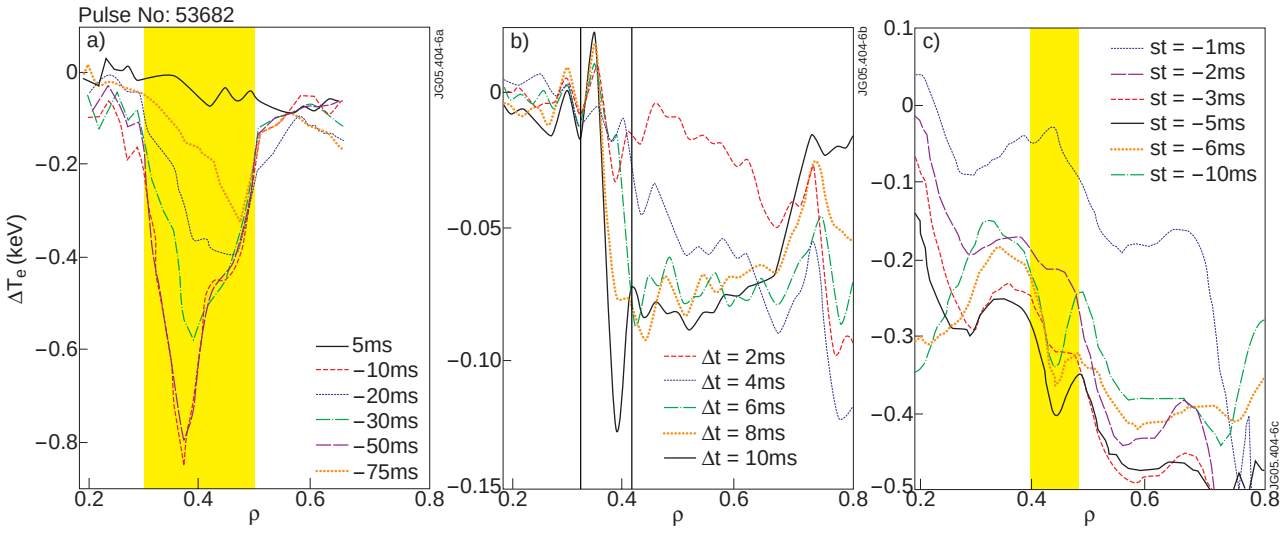

Figure 6: (colors on-line): Time evolution of experimental (a) and simulated (b,c) T_e variation (ΔT_e) profile following a cold pulse in ITB plasma. (b) with TRB, (c) with CUTIE.

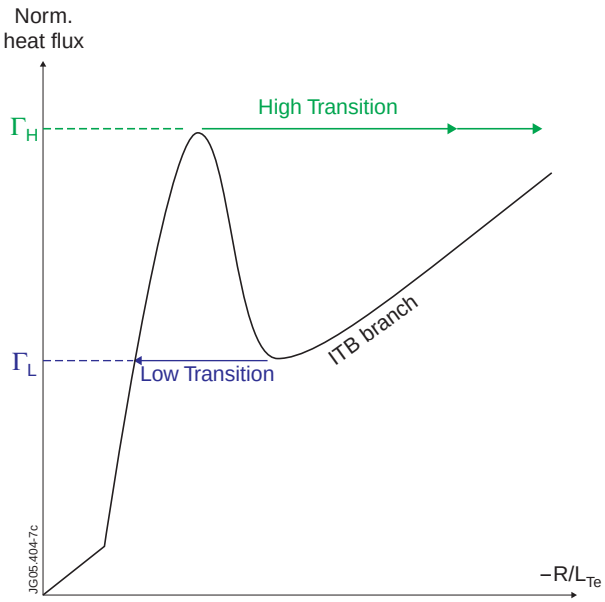

Figure 7: (colors on-line). Schematic of 1nd order transition for ITB formation.

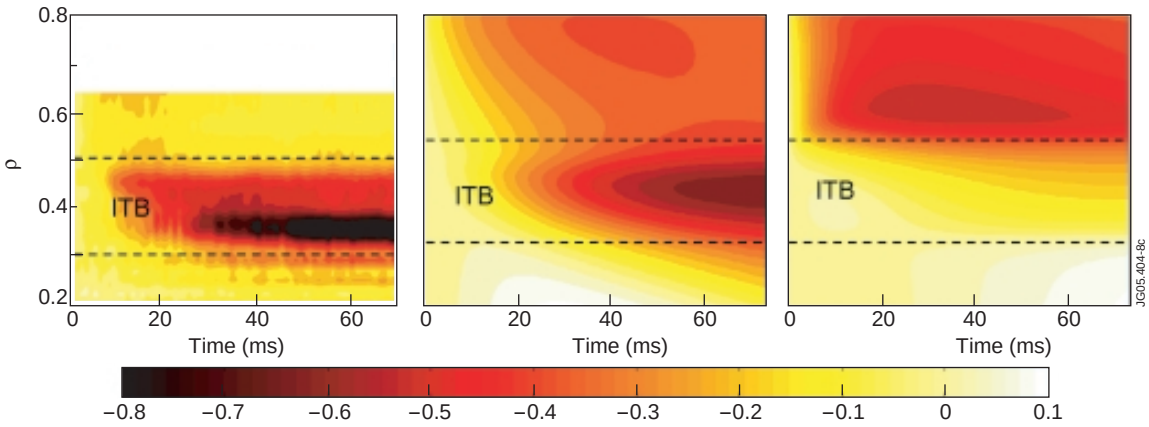

Figure 8: (colors on-line). Contour plots of ΔT_e during cold pulse in ITB plasma: (a) experimental Pulse No: 53682; (b) simulated with an empirical 2nd order transition model (as in Fig.4), (c) simulated with an empirical 1nd order transition model (as in Fig.7). Units of ΔT_e color codes are keV. t=0ms corresponds to the application of the cold pulse in the edge region.